Transit Met Chem
DOI 10.1007/s11243-017-0159-3

# Copper(II)-complex functionalized magnetite nanoparticles: a highly efficient heterogeneous nanocatalyst for the synthesis of 5-arylidenthiazolidine-2,4-diones and 5-arylidene-2-thioxothiazolidin-4-one

**Malihe Akhavan[1] · Naser Foroughifar[1] · Hoda Pasdar[1] · Alireza Khajeh-Amiri[2] · Ahmadreza Bekhradnia[3]**

Received: 22 March 2017 / Accepted: 26 June 2017


**Abstract** Magnetite nanoparticles (MNPs) have proved to be a useful support for heterogeneous catalysis. We have synthesized $Fe_3O_4$ MNPs functionalized with a copper(II) complex, and tested the resulting material as a heterogeneous nanocatalyst. The catalyst was tested for aldol condensation reactions between aliphatic/aromatic aldehydes and rhodanine or thiazolidine-2,4-dione (TZD) derivatives under reflux in ethanol, giving the target products in high yield. Environmentally benign chemistry, short reaction times, simple work-up, excellent yields, and the reusability of the new nanocatalyst are beneficial features of the present study. The nanocatalyst was characterized by scanning electron microscopy, vibrating sample magnetometery, thermogravimetry, X-ray diffraction, and energy-dispersive X-ray analyses. The data showed that the magnetic nanoparticles are super-paramagnetic with a size range of 10–20 nm.

**Electronic supplementary material** The online version of this article (doi:10.1007/s11243-017-0159-3) contains supplementary material, which is available to authorized users.

✉ Naser Foroughifar
n_foroughifar@yahoo.com

[1] Department of Chemistry, Tehran North Branch, Islamic Azad University, Tehran, Iran

[2] Young Researchers and Elites club, Yadegar-e Imam Khomeini (RAH) Shahre Rey Branch, Islamic Azad University, Tehran, Iran

[3] Department of Medicinal Chemistry and Pharmaceutical Sciences Research Center, Mazandaran University of Medical Sciences, Sari, Iran

## Introduction

Five-membered heterocycles including the thiazole nucleus with two heteroatoms and a carbonyl group on the fourth carbon, such as rhodanine and thiazolidine-2,4-dione derivatives, have a wide spectrum of biological and pharmacological activities [1, 2]. In the past two decades, these compounds have been found to possess antitumor, anti-inflammatory, anti-microbial, and antidiabetic properties, and have found clinical use in medications such as ciglitazone, englitazone, rosiglitazone, pioglitazone, epalrestat, and troglitazone for the treatment of type 2 diabetes mellitus. They are also key intermediates for the synthesis of anti-HIV and anti-ischemic agents [3–5]. Hence, the molecular modification and pharmacological evaluation of these molecules have attracted much attention from synthetic chemists and pharmacologists [4].

Because of pharmacological and medicinal importance of rhodanine and thiazolidine-2,4-dione, numerous methods have been applied for the synthesis of these compounds and their derivatives, with an extensive range of catalysts including Alum [6], ionic liquids [7], glycine and sodium carbonate [8], piperidinium acetate [9], and piperidine [10]. However, currently known methods suffer from one or more drawbacks, such as low yields, long reaction times, tedious work-up procedures, toxic residues, special apparatus, environmentally unfavorable solvents, and a requirement for excess catalyst. Also, using the amine was found to be carcinogenic and problematic in the recovery and reusability of the catalysts [11, 12].

Although homogeneous catalysts can provide excellent activity and selectivity for a variety of reactions, the problems of catalyst separation from the product mixture and use of large amounts of organic solvents are the main weaknesses in their wider industrial utility [13, 14].

Published online: 04 July 2017

According to the principles of green chemistry, magnetic nanoparticles (MNPs) offer features such as easy preparation and functionalization, considerable durability and reusability, high surface area, low toxicity, and facile recovery with the aid of an external magnet [15, 16]. Consequently, the cost of the desired product can be significantly diminished by the use of MNP catalysts. Moreover, the heterogenization of homogeneous catalysts on solid supports is a significant field of research in catalysis.

In recent years, functionalized MNPs have been used in magnetic resonance imaging, drug delivery systems, cell biology, biotechnology, protein separation, and cancer treatments [17, 18]. They have also been applied in various organic reactions such as Knoevenagel condensation, Suzuki and Heck cross-coupling, asymmetric aldol reaction, asymmetric hydrogenation of aromatic ketones, reduction of nitro aromatic compounds, cyanosilylation of carbonyl compounds, and enantioselective direct addition of terminal alkynes to imines [19]. Thus, homogeneous catalysts have various benefits but heterogeneous catalysts are widely applied due to their easy recovery [20]. The advantages of magnetic heterogeneous catalysts, especially involving copper supported on MNPs, include efficiency, enhanced stability and magnetic retrieval and reuse of the catalyst [21].

Recently, a copper(II)-catalyst for the Michael–aldol reaction has been developed [22]. However in spite of high yields, recycling problems have limited its development. Therefore, to minimize these disadvantages, the heterogenization of homogeneous catalysts has emerged as a research focus [23]. With the aim to develop a more efficient catalyst, we herein describe aldol condensation reactions using various aldehydes and rhodanine or thiazolidine-2,4-dione in the presence of a magnetically reusable and efficacious $Fe_3O_4$@$SiO_2$-$NH_2$/Cu(II) catalyst under Knoevenagel condensation conditions. To the best of our knowledge, the use of nanoparticle-supported copper (II) catalysts for the one-pot synthesis of 5-arylidenthiazolidine-2,4-diones and 5-arylidene-2-thioxothiazolidin-4-one has not been previously reported.

## Experimental

### Materials and instrumentation

All solvents and reagents were purchased from Merck and used without additional purification. FTIR spectra were obtained in the region of 400–4000 $cm^{-1}$ as KBr pellets with a PerkinElmer 550 spectrometer. Melting points were recorded with an Electrothermal 9200 apparatus and are not corrected. Known products were identified by comparison of their melting points and spectral data with those reported in the literature. $^1$HNMR (400 MHz) and $^{13}$CNMR (100 MHz) spectra were recorded with a Bruker Advance spectrometer with $CDCl_3$ or DMSO-$d_6$ as solvent and TMS as an internal standard. TLC was performed on silica gel poly gram SILG/UV 254 nm plates. The X-ray diffraction (XRD) pattern of the catalyst was recorded with an X-Pert Pro instrument (Cu kα radiation, $\lambda = 1.54$ A) in the region of $2\Theta = 20°–80°$. Magnetite properties of the nanocatalyst were analyzed using a varying magnetic field from −10000 to 10000 on a BHV-S5 vibrating sample magnetometer (VSM). Thermogravimetric analysis curves were carried out using a PL-STA 1500 device manufactured by Thermal Sciences. Thermal analyzer with heating rate of 10 °C $min^{-1}$ over a temperature limited area of 30–1300 °C under $N_2$ atmosphere. Morphology was analyzed by SEM (Hituch S4160 scanning electron microscope).

### Preparation of $Fe_3O_4$ MNPs

$Fe_3O_4$ MNPs were synthesized via co-precipitation of $Fe^{3+}$ and $Fe^{2+}$ in ammonia solution as follows [24]. $FeCl_3{\cdot}6H_2O$ (0.86 g, 3.2 mmol) and $FeCl_2{\cdot}4H_2O$ (0.31 g, 1.6 mmol) were dissolved in distilled water (300 ml). The solution was stirred at 90 °C for 1 h under $N_2$ atmosphere. Then ammonia solution was added dropwise until pH 11, and the suspension was stirred for 1 h. The prepared $Fe_3O_4$ MNPs were isolated from the mixture by applying an external magnet, washed several times with water, and dried in vacuum at 60 °C for 5 h.

### Preparation of $Fe_3O_4$@$SiO_2$

Silica-coated magnetite nanoparticles were prepared by the Stöber method [24]. $Fe_3O_4$ MNPs (1 g) were dispersed in a mixture of ethanol (33 ml), distilled water (9 ml), and concentrated ammonia solution 25% (0.7 ml) by ultrasonic bath for 30 min. Thentetraethyl orthosilicate (TEOS) (0.5 ml) was then added dropwise. After vigorous stirring for 24 h at room temperature, the solid was magnetically separated, washed sequentially with water (3 × 100 ml) then ethanol (3 × 100 ml), and dried in vacuum at 60 °C for 5 h.

### Preparation of $Fe_3O_4$ @$SiO_2$-Cl

$Fe_3O_4$@$SiO_2$-Cl nanoparticles were synthesized with slight modification of the literature procedure [24]. To a suspension of $Fe_3O_4$@$SiO_2$ (1 g) in dry toluene (100 ml), 3-chloropropyltrimethoxysilane (CPTMS) (1 ml) was added and the mixture was sonicated for 30 min under $N_2$ atmosphere. Then, the mixture was stirred for 12 h under reflux and the resulting solid ($Fe_3O_4$/$SiO_2$-Cl) was

separated and washed with toluene (3 × 100 ml) then ethanol (3 × 100 ml) and finally dried under vacuum at 60 °C for 5 h.

### Preparation of $Fe_3O_4$@$SiO_2$-$NH_2$

$Fe_3O_4$@$SiO_2$-$NH_2$ nanoparticles were synthesized by a modified literature procedure [24]. $Fe_3O_4$@$SiO_2$-Cl (1 g) was suspended in acetonitrile (100 ml) with sonication for 30 min. Then, KI (0.27 g, 7 mmol) and $K_2CO_3$ (0.96 g, 7 mmol) were added and the mixture was sonicated for 30 min. Next, 1,3-diaminopropane (0.52 g, 20 mmol) was added under stirring and the mixture was refluxed for 10 h. The resulting solid was separated magnetically, washed with water/ethanol (20 ml/20 ml), and dried under vacuum at 60 °C for 5 h.

### Preparation of $Fe_3O_4$@$SiO_2$-$NH_2$/Cu(II)

$Fe_3O_4$@$SiO_2$-$NH_2$ (1 g) was added to a solution of $Cu(OAc)_2.H_2O$ (0.29 g, 1.5 mmol) in ethanol (50 ml). The mixture was sonicated for 30 min, then refluxed for 10 h. The separated $Fe_3O_4$@$SiO_2$-$NH_2$/Cu(II) was washed with methanol and dried under vacuum at 60 °C for 5 h.

### Preparation of 2,4-thiazolidinedione

Chloroacetyl chloride (7.02 g, 60 mmol) and thiourea (4.56 g, 60 mmol) were dissolved in distilled water (10 ml). The mixture was stirred for 20 min to form a white precipitate. Concentrated hydrochloric acid (6 ml) was then added and the mixture refluxed for 7–8 h. The product was filtered off, washed with water (20 ml), and dried under vacuum. Yield 6.61 g (90%).

### Preparation of rhodanine

Carbon disulfide (5 ml) was added to ammonia solution (5 ml), and the reaction mixture was stirred for 30 min at 40 °C. The resulting ammonium dithiocarbamate solution was added to a solution of sodium chloroacetate in distilled water over 5 min. The reaction mixture was allowed to stand for 20–30 min, then added to boiling *6 N* hydrochloric acid (10 ml) and heated at 100–110 °C. The precipitate was filtered off, washed with water (30 ml), and dried under vacuum. Yield 10.28 g (94%).

### General procedure for aldol condensation

To a mixture of thiazolidine-2,4-dione or rhodanine (0.13 g, 1 mmol), aliphatic/aromatic aldehyde (1 mmol), and ethanol (4 ml), a portion of $Fe_3O_4$@$SiO_2$-$NH_2$/Cu(II) (0.15 g) was added and the mixture stirred under reflux for the required time (Table 2). The progress of the reaction was monitored by TLC (n-hexane/EtOAc, 2:1). After completion of the reaction, EtOH (3 ml) was added and the nanocatalyst was separated by an external magnet. The crude product was recrystallized from EtOH.

### Spectroscopic data for the compounds

Thiazolidine-2,4-dione White crystals (94%); m.p. 126–127 °C; IR: 3468(M), 3444(M), 2963(W), 2823(W), 1736 (S), 1653(S), 1391(W), 1341(M), 1227(M), 1162(S), 890 (M), 806(M), 788(M), 715(M), 617(M), 513(M) $cm^{-1}$; $^1$H-NMR (400 MHz,$CDCl_3$): δ (ppm) 4.07 (s, 2H, CH2), 8.66 (brs, 1H, NH); $^{13}$C-NMR (100 MHz, $CDCl_3$):38.6, 169.2, 173.5.

2-thioxo-thiazolidine-4-one (rhodanine) Yellow crystals (92%); m.p. 168–169 °C; IR: 3468(W), 3135(W), 3039 (W), 2703(W), 1731(S), 1643(S), 1395(M), 1347(M), 1205 (M), 1174(M), 897(W), 876(W), 788(W), 787(W), 662(W), 542(W) $cm^{-1}$; $^1$H-NMR (400 MHz, $CDCl_3$): δ (ppm) 4.26 (s, 2H, CH2), 12.88 (bs, 1H, NH); $^{13}$C-NMR (100 MHz, $CDCl_3$): 40.6, 175.5, 201

(Z)-5-Benzylidene-thiazolidine-2,4 -dione(**1a**) m.p. 251–252 °C; IR: 3459(W), 3899(M), 1688 (S), 600-800 (W), 3136 (S) $cm^{-1}$; $^1$H-NMR (400 MHz, DMSO-$d_6$): δ (ppm) 7.52–7.61 (m, 5H, ArH), 7.2 (s, 1H, = CHAr), 10.62 (brs, 1H, NH); $^{13}$C-NMR (100 MHz, DMSO-*$d_6$*):125.3, 127.9, 131.7130, 137, 143.5, 168.3, 170.1

(Z)-5-Benzylidene-2-thioxo-thiazolidine-4-one (**2a**) m.p. 210–212 °C; IR: 3193(M), 1237(M), 1728(S), 600-800(W), 3018(S) $cm^{-1}$; $^1$H-NMR (400 MHz, DMSO-*$d_6$*): δ (ppm) 7.50–7.60 (m, 5H, ArH),7.7 (s, 1H, = CHAr), 10.89 (bs, 1H, NH); $^{13}$C-NMR (100 MHz, DMSO-*$d_6$*):124.9, 128.1, 132.2, 130.1, 136.8, 143.9, 168.9, 196.5

(Z)-5-(4-Methoxybenzylidene)-thiazolidine-2,4-dione (**3b**) m.p. 218–220 °C; IR: 3383 (M), 1732(M), 1694(S), 600–800(W), 3218(S), 1184(M) $cm^{-1}$; $^1$H-NMR (400 MHz, $CDCl_3$): δ (ppm) 3.89 (s, 3H, $OCH_3$), 7.01 (m, 2H, ArH), 7.49 (m, 2H, ArH), 7.83 (s, 1H, = CHAr), 8.36 (brs, 1H, NH); $^{13}$C-NMR (100 MHz, $CDCl_3$): 56.5, 114.9, 116.4, 128.1, 128.8, 142.8, 160.1, 167.2, 168.9

(Z)-5-(4-Methoxybenzylidene)-2-thioxo-thiazolidine-4-one (**4b**) m.p. 235–237 °C; IR:3353 (M), 1686(S), 1221(M), 600–800(W),3158(S), 1174(M) $cm^{-1}$; $^1$H-NMR (400 MHz, $CDCl_3$): δ (ppm) 3.84 (s, 3H, $OCH_3$),7.3 (m, 2H, ArH), 7.58 (m, 2H, ArH), 7.91 (s, 1H, = CHAr), 8.72 (brs, 1H, NH); $^{13}$C-NMR (100 MHz, $CDCl_3$): 56.8, 115.1, 116.8, 129.3, 129, 143.1, 161.2, 168.9, 196.3

(Z)-5-(4-Hydroxybenzylidene)-thiazolidine-2,4-dione (**5c**) m.p. 298–299 °C; IR:3344 (M), 1721(S), 600-800(W),

3113(S), 3160(S) $cm^{-1}$; $^{1}$H-NMR (400 MHz, DMSO-$d_6$): δ (ppm) 6.98 (m, 2H, ArH), 7.58 (m, 2H, ArH), 7.86 (s, 1H, = CHAr), 7.28 (s, 1H, ArOH), 10.42 (bs, 1H, NH); $^{13}$C-NMR (100 MHz, DMSO- $d_6$):114.7, 116.5, 127.7, 128.9, 146, 160.5, 167.9, 168.7

(Z)-5-(4-Hydroxybenzylidene)-2-thioxo-thiazolidine-4-one (**6c**) m.p. 288–290 °C; IR:3341 (M), 1688 (S), 1173 (M), 600-800 (W),3120 (S), 3161 (S) $cm^{-1}$; $^{1}$H-NMR (400 MHz, DMSO-$d_6$): δ (ppm) 7.2 (m, 2H, ArH), 7.63 (m, 2H, ArH), 7.86 (s, 1H, = CHAr), 7.44 (s, 1H, ArOH), 10.7 (bs, 1H, NH); $^{13}$C-NMR (100 MHz, DMSO-$d_6$):115.8, 116.9, 128.0, 129.7, 145.0, 160.0, 167.5, 196.4

(Z)-5-(1H-Indol-3- yl methylene)-thiazolidine-2, 4- dione (**7d**) m.p. 185–186 °C; IR:3225(M), 1687(S), 600-800 (W), 3112(S) $cm^{-1}$; $^{1}$H-NMR (400 MHz, DMSO-$d_6$): δ (ppm) 6.99 (s, 1H, = CHAr), 7.019 (m, 1H, ArH), 7.38 (m, 1H, ArH), 7.54 (m, 1H, ArH) 7.71(m, 1H, ArH), 12.01 (brs, 1H, NH), 13.2 (brs, 1H, NH(indole)); $^{13}$C-NMR (100 MHz, DMSO-$d_6$): 110, 111.1, 119, 120.1, 121.9, 122.2, 126.0, 130.8, 135.0, 143.5, 167.3, 168.1

(Z)-5-(1H-Indol-3-yl-methylene)-2-thioxo-thiazolidine-4-one(**8d**) m.p. 306–307 °C; IR: 3235 (M), 1716(S), 1178 (M), 600–800(W), 3053(S)$cm^{-1}$; $^{1}$H-NMR (400 MHz, DMSO-$d_6$): δ (ppm) 6.99 (s, 1H, = CHAr), 7.09 (m, 1H, ArH), 7.37 (m, 1H, ArH), 7.54 (m, 1H, ArH) 7.71(m, 1H, ArH), 11.01 (bs, 1H, NH), 13.02 (brs, 1H, NH(indole)); $^{13}$C-NMR (100 MHz, DMSO-$d_6$): 108.6, 11.8, 1203, 121.3, 122.3, 124.5, 126.8, 128.8, 136.1, 144, 168.3, 194.6

(Z)-5-((Thiophen -2-yl) methylene)-thiazolidine-2,4- dione (**9e**) m.p. 240–242 °C; IR:3198(M), 1727(S), 665 (W) 3056(S) $cm^{-1}$; $^{1}$H-NMR (400 MHz, DMSO-$d_6$): δ (ppm), 7.27 (d, 1H, ArH), 7.43 (d, 1H, ArH), 7.69 (d, 1H), 8.05(s, 1H, = CH), 13.67 (s, 1H, NH); $^{13}$C-NMR (100 MHz, DMSO-$d_6$): 123.1, 124.8, 129.3, 134.37, 135.44, 137.5, 167.5, 169.9

(Z)-5-((Thiophen-2-yl) methylene)-2-thioxothiazolidin-4-one (**10e**) m.p. 214–215 °C; IR:3128(M), 1728(S), 1171 (M), 667(W) 3055(S) $cm^{-1}$; $^{1}$H-NMR (400 MHz, DMSO-$d_6$): δ (ppm): 7.27 (d,1H, ArH),7.68 (d,1H, ArH), 7.90 (d, 1H, ArH), 8.02(s, 1H, = CH), 10.07 (s, 1H, NH); $^{13}$C-NMR (100 MHz, DMSO-$d_6$): 123.1, 124.8, 129.3, 134.3, 135.4, 137.5, 168.1, 194.4

(Z)-5-(2-Chlorobenzylidene)-2-thioxothiazolidin-4-one (**11f**) m.p. 218–220 °C; IR:3033(M), 1694(S), 1189(M), 1581 (M), 1465(M), 849(S), 1038(W), 2829(S) $cm^{-1}$; $^{1}$H-NMR (400 MHz, DMSO-$d_6$): δ (ppm) 7.23–7.48 (m, 4H, Ar–CH), 7.79–7.91 (s, 1H, = CH), 13.7 (brs, 1H, NH); $^{13}$C-NMR (100 MHz, DMSO-$d_6$): 116.1, 126.5, 127.5, 129.4, 129.9, 133.4, 143.5, 168.7, 193.5

(Z)-5-(2-Chlorobenzylidene) thiazolidine-2,4- dione (**12f**) m.p. 182–183 °C; IR:3420(M), 1741(S), 1581(M), 841(S), 2829(S) $cm^{-1}$; $^{1}$H-NMR (400 MHz, DMSO-$d_6$): δ (ppm): 7.93 (s, 1H, = CH), 7.45-7.93 (m, 4H, Ar–CH), 12.90 (brs, 1H, NH); $^{13}$C-NMR (100 MHz, DMSO-$d_6$): ppm 116.5, 127.2, 128.6, 130.1, 131.4, 132.8, 134.4, 167.9172.8

(Z)-5-(4-Flurobenzylidene)-thiazolidine-2, 4-dione (**13g**) m.p. 223–224 °C; IR:3203(M), 1724(S), 3023(S), 1125 (S) $cm^{-1}$; $^{1}$H-NMR (400 MHz, DMSO-$d_6$): δ (ppm): 7.41 (m, 2H, ArH), 7.73 (m, 2H, ArH), 7.84 (s, 1H, = CHAr), 12.56 (br s, 1H, NH); $^{13}$C-NMR (100 MHz, DMSO-$d_6$): 116, 115.9 (2C), 129.5 (2C), 131.3, 140.5, 164.5, 168.1169.0

(Z)-5-(4-Flurobenzylidene)-2-thioxo-thiazolidine-4-one (**14g**) m.p. 219–220 °C; IR:3210(M), 1235(M), 1694(S), 1580 M (S), 1120(S) $cm^{-1}$; $^{1}$H-NMR (400 MHz, DMSO-$d_6$): δ (ppm): 7.38 (m, 2H, ArH), 7.71 (m, 2H, ArH), 7.67 (s, 1H, = CHAr), 13.50 (brs, 1H, NH); $^{13}$C-NMR (100 MHz, DMSO-$d_6$): ppm 116.4, 115.9 (2C), 129.5 (2C), 131.3, 140.5, 165.5, 169.7, 191.8.2.8.17

(Z)-5-((Quinoxalin-3-yl) methylene) thiazolidine-2,4-dione (**15h**) m.p. 288–290 °C; IR:3452(M), 1732(S), 2964(S), 1398(M),2919(S) $cm^{-1}$; $^{1}$H-NMR (400 MHz, DMSO-$d_6$): δ (ppm): 7.92-8.17(m, 4H, ArH), 7.59 (s, 1H, = CHAr), 9.31 (s, 1H, = CHN), 12.65 (brs, 1H, NH); $^{13}$C-NMR (100 MHz, DMSO-$d_6$): ppm 124.06, 129.27, 129.48, 129.6, 131.73, 131.4, 141.76, 142.25, 1438.1, 148.8, 167.3, 168.5

(Z)-5-((Quinoxalin-3-yl) methylene)-2-thioxothiazolidinone (**16h**) m.p. 295–296 °C; IR:3321(M),1654(M), 1732 (S), 2094(S), 1395(M) $cm^{-1}$; $^{1}$H-NMR (400 MHz, DMSO-$d_6$): δ (ppm) 7.91-8.16(m, 4H, ArH), 7.5 (s, 1H, = CHAr), 9.30 (s, 1H, = CHN), 12.60 (brs, 1H, NH); $^{13}$C-NMR (100 MHz, DMSO- $d_6$): ppm 124.05, 129.27, 129.48, 129.5, 131.71, 131.2, 141.75, 142.24, 143.2, 148.75, 168.3, 192.5

(Z)-5-((Naphthalen-3-yl) methylene)-2-thioxothiazolidin-4- one (**17i**) m.p. 270–272 °C; IR: 3132(M), 1648(M), 1732(S), 1479(M), 2684(S) $cm^{-1}$; $^{1}$H NMR (400 MHz, $CDCl_3$): δ (ppm) 7.71–7.82 (m, 3H), 8.10–8.15 (m, 4H), 8.60 (s, 1H), 11.77 (brs, 1H, NH); 13C-NMR (100 MHz, $CDCl_3$): δ (ppm) 123.6, 125.8, 127.3, 127.5, 127.8, 128.7, 128.8, 130.5, 130.7, 131.5, 132.6, 133.1, 167.8, 192.7

(Z)-5-((Naphthalen-3-yl) methylene) thiazolidine-2, 4-dione (**18i**) m.p. 252–253 °C; IR:3223(M), 1739(S), 1698 (S), 1580(M),2094(S) $cm^{-1}$; $^{1}$H-NMR (400 MHz, $CDCl_3$): δ (ppm) 7.70–7.76 (m, 3H), 7.94–8.08 (m, 4H), 8.50 (s, 1H), 12.65 (brs, 1H, NH); $^{13}$C-NMR (100 MHz, $CDCl_3$):δ (ppm) 123.7, 125.9, 127.1, 127.6, 127.9, 128.6, 128.9, 130.6, 130.8, 131.7, 132.7, 133.2, 167.5, 168.9

(Z)-5-(3-Methylbutylidene) thiazolidine-2,4 -dione (**19j**) m.p. 166–167 °C; IR:3343 (M), 1732(S), 1685 (S), 2963 (W) $cm^{-1}$;$^{1}$H-NMR (400 MHz, $CDCl_3$): δ (ppm) 1.21 (d, 6H), 1.78–1.82 (m, 1H), 2.17–2.18 (m, 2H), 6.82 (t, 1H), 8.67 (brs, 1H, NH); $^{13}$C-NMR (100 MHz, $CDCl_3$): 25.51 (2C), 27.55, 40.25, 70.91, 126.01, 136.1, 166.95, 167.63

(Z)-5-(3-Methylbutylidene)-2-thioxothiazolidin-4- one (**20j**) m.p. 188–189 °C; IR: 3142 (M), 1655(M), 1725(S), 2964 (W) $cm^{-1}$;$^{1}$H-NMR (400 MHz, DMSO-$d_6$): δ (ppm) 1.2–1.22(d, 6H), 1.74–1.82 (m, 1H), 2.17–2.18 (m, 2H), 6.92–6.88 (t, 1H), 9.4 (brs, 1H); $^{13}$C-NMR (100 MHz, DMSO-$d_6$): 25.5 (2C), 27.5, 40.2, 70.9, 126.0, 136.0, 167.9, 192.6

## Results and discussion

### Catalyst preparation and characterization

The new magnetically recoverable catalyst $Fe_3O_4$@$SiO_2$-$NH_2$/Cu (II) was prepared as shown in (Scheme 1). Firstly, $Fe_3O_4$ (MNPs) were synthesized by co-precipitation of $Fe^{2+}$ and $Fe^{3+}$ from ammonia solution. The surface of the $Fe_3O_4$ MNPs was then coated with a silica shell by the hydrolysis and condensation of tetraethyl orthosilicate in ethanol/ammonia mixture to produce $Fe_3O_4$@$SiO_2$. Next, chloropropyl modified $Fe_3O_4$@$SiO_2$ ($Fe_3O_4$@$SiO_2$-Cl), $Fe_3O_4$@$SiO_2$ was prepared by reaction of chloropropyl triethoxysilane. $Fe_3O_4$@$SiO_2$-$NH_2$ was synthesized via the substitution of $Fe_3O_4$@$SiO_2$-Cl with excess 1,3-propanediamine. Finally, complexation of the $Fe_3O_4$@$SiO_2$-$NH_2$ was performed by reaction with excess Cu $(OAc)_2$·$H_2O$.

### FTIR spectroscopy

FTIR spectra of $Fe_3O_4$, $Fe_3O_4$@$SiO_2$, $Fe_3O_4$@$SiO_2$-Cl, $Fe_3O_4$@$SiO_2$-$NH_2$ and $Fe_3O_4$@$SiO_2$-$NH_2$/Cu(II) are shown in Fig. 1. The band at 573 $cm^{-1}$ is typical of structural Fe–O vibrations. A broad absorption band at 3386 $cm^{-1}$ is assigned to –OH groups on the $Fe_3O_4$ surface (Fig. 1a). For the $Fe_3O_4$@$SiO_2$ nanoparticles, a sharp band at 1072 $cm^{-1}$ is attributed to Si–O-Si asymmetric stretching vibrations, indicating the presence of a $SiO_2$ layer around the $Fe_3O_4$ core. Peaks at around 960 and 3736 $cm^{-1}$ are assigned to Si–OH moieties (Fig. 1b). The presence of C-H stretching modes assigned to the propyl groups in Fig. 2c, d is confirmed by stretching vibrations at about 1459 and 2927 $cm^{-1}$, while peaks at 3421 and 1508–1551 $cm^{-1}$ are assigned to the stretching and bending vibrations of the amino groups (Fig. 1c, d). The band at 1551 $cm^{-1}$ shifted to lower frequency 1504 $cm^{-1}$, upon reaction of the amine with $Cu(OAc)_2$. Also, new absorption bands at 516 and 470 $cm^{-1}$ are assigned to Cu–N and Cu–NH bands (Fig. 1e), suggesting that the $Fe_3O_4$@$SiO_2$-$NH_2$/Cu(II) was synthesized successfully.

### XRD study

The crystalline structure of $Fe_3O_4$@$SiO_2$-$NH_2$/Cu(II) was examined by X-ray diffraction (Fig. 2). According to Fig. 2, diffraction peaks observed at 2Θ = 30.1°, 35.6°,

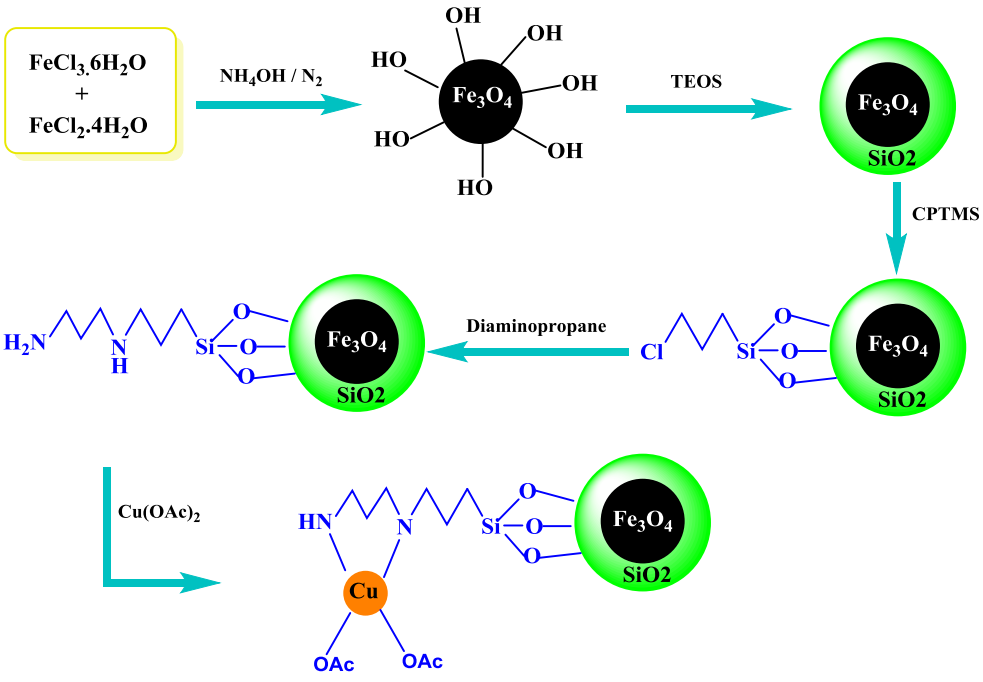


**Scheme 1** Synthetic pathways for the synthesis of $Fe_3O_4$@$SiO_2$-$NH_2$/Cu(II)

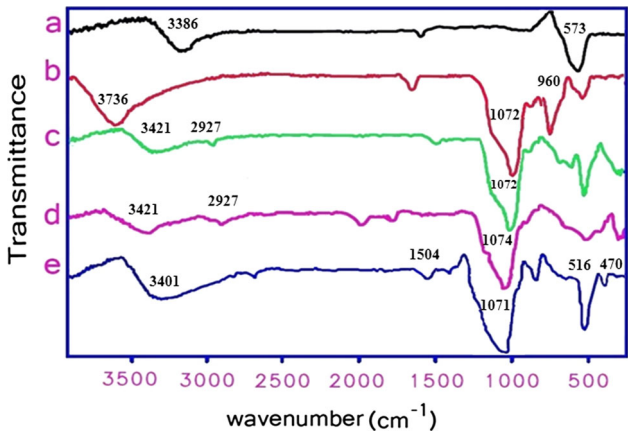


**Fig. 1** FTIR spectra of (*a*) $Fe_3O_4$ NPs (*b*) $Fe_3O4/SiO_2$ (*c*) $Fe_3O_4/SiO_2$-Cl (*d*) $Fe_3O_4/SiO_2$-$NH_2$ (*e*) $Fe_3O_4$@$SiO_2$-$NH_2$/Cu(II) (KBr pellet)

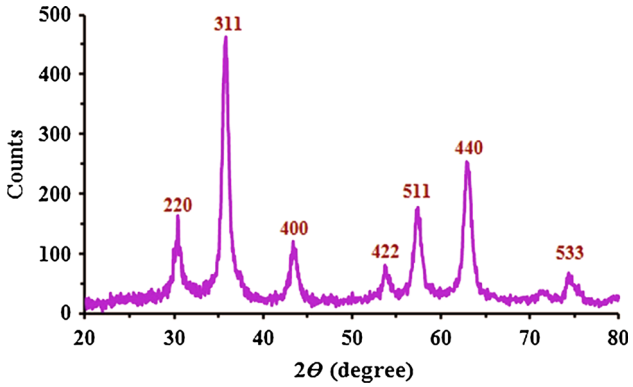


**Fig. 2** XRD diffraction pattern of $Fe_3O_4$@$SiO_2$-$NH_2$/Cu(II)

43.3º, 53.7º, 57.2º, 63.1º, 74.2º can be assigned to the (220), (311), (400), (422), (511), (440) and (533) planes of $Fe_3O_4$, respectively, matching well with the standard patterns of spinel ferrites available in the literature (JCPDS file No. 19-0629). This shows the survival of the crystalline spinel ferrite core structure during the $Fe_3O_4$@$SiO_2$-$NH_2$/Cu(II) coating process. Through the Debye–Scherrer formula ($D = K\,\lambda/\beta\cos\Theta$), the average crystalline size of $Fe_3O_4$@$SiO_2$-$NH_2$/Cu (II) particles was determined. D, k, λ, β, Θ in this formula, signify mean grain size, Scherrer's constant, X-ray wavelength, corrected diffraction line full-width at half-maximum (FWHM) and Bragg diffraction angle, respectively. The average size of $Fe_3O_4$@$SiO_2$-$NH_2$/Cu(II) was determined as about 13 nm for the width of the peak at $2\Theta = 35.6º$ (311), which is smaller than the value determined by SEM analysis.

## SEM study

Scanning electron microscopy is very useful for the characterization of surface morphology and size of the MNPs. The SEM image of the as-prepared $Fe_3O_4$@$SiO_2$-$NH_2$/Cu (II) is shown in Fig. 3. The particles have a mean diameter of about 13-20 nm, and most are almost spherical in shape.

## EDAX study

EDAX analysis was used to get some information on the elemental composition and distribution on the surface of the $Fe_3O_4$@$SiO_2$-$NH_2$/Cu(II). Thus, Fe, O, Si, C, N, and Cu were detected based on the results in Fig. 4. The obvious presence of a Cu signal in the EDAX spectrum demonstrates that Cu(II) was immobilized onto the surface of the diamine-functionalized MNPs. According to the above analysis, it can be concluded that the $Fe_3O_4$@$SiO_2$-$NH_2$/Cu(II) MNPs have been successfully synthesized.

## TGA study

The stability of the $Fe_3O_4$@$SiO_2$-$NH_2$/Cu(II) and the bond formation between $Fe_3O_4$@$SiO_2$-$NH_2$ and copper(II) were

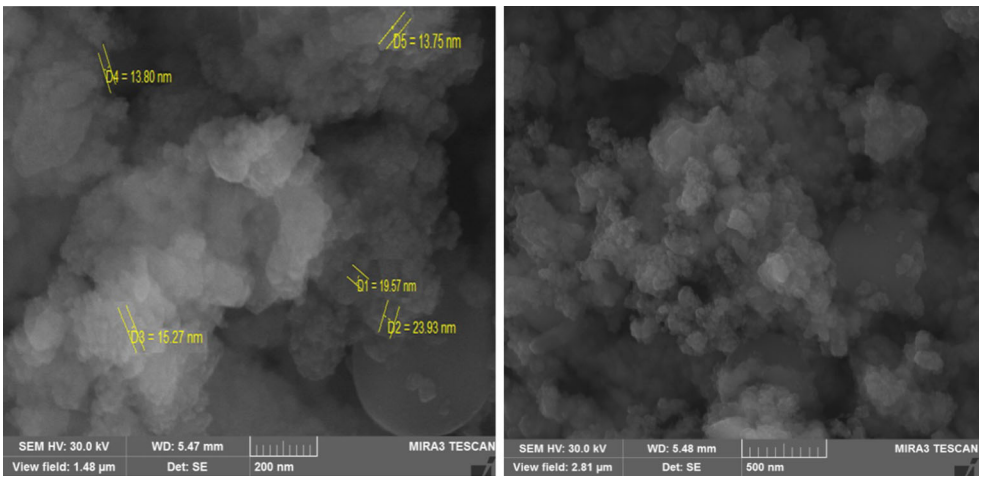


**Fig. 3** SEM images of $Fe_3O_4$@$SiO_2$-$NH_2$/Cu(II)

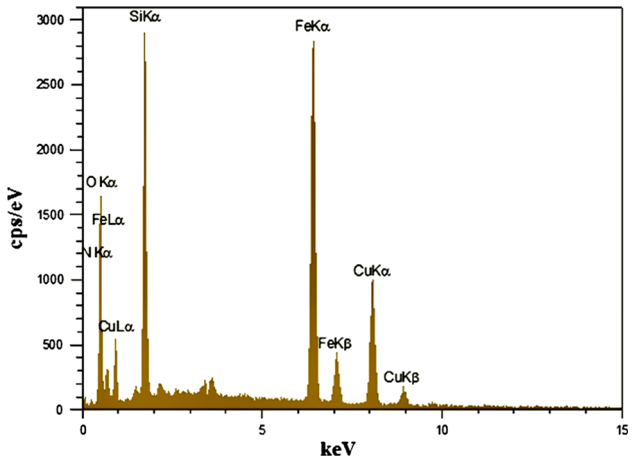


**Fig. 4** Energy-dispersive X-ray (EDX) spectrum of $Fe_3O_4$@$SiO_2$-$NH_2$/Cu(II)

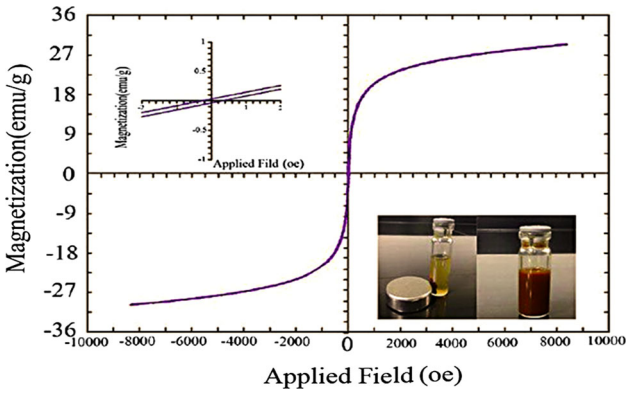


**Fig. 6** Magnetization curves of $Fe_3O_4$@$SiO_2$-$NH_2$/Cu(II). Left inset: the magnified field from −3 to 3 Oe. Right inset: dispersal of the MNPs in solvent and capture by an external magnet

examined by thermogravimetric analysis (Fig. 5). The TGA measurements were taken using a weighed powder sample of 5–10 mg in a platinum pan, with the results shown in Fig. 5. The sample was heated from 30 to 1300 °C at a heating rate 15 °C/min under a nitrogen stream. The weight loss below 230 °C is attributed to loss of adsorbed water and or water formed by the condensation of hydroxyl groups [25]. A weight loss at approximately 230–650 °C is attributed to decomposition of organic groups grafted to the surface the MNPs. A weight loss between 650 and 1218 °C can be ascribed to the decomposition of the residual structure. According to the TGA curve, the amount of organic moiety was about 5.5% and inorganic moiety was about 4.5% against the total heterogeneous catalyst [25].

## Magnetic study

The magnetic properties of the $Fe_3O_4$@$SiO_2$-$NH_2$/Cu(II) MNPs were determined using a vibrating sample magnetometer (VSM) at room temperature (Fig. 6). The hysteresis curve allows designation of the saturation magnetization (Ms), coercivity (Hc), and remanent magnetization (Mr). According to Fig. 6, the saturation magnetization quantity was 27 emu/g. Hence because of the silica coating, the functionalized magnetic nanoparticles have a lower magnetic quantity compared with bar magnetic nanoparticles (74.3 emu/g). On the basis of Fig. 6 (left inset), we can also see that Mr and Hc are negligible; hence, the $Fe_3O_4$@$SiO_2$-$NH_2$/Cu(II) MNPs can be regarded as super-paramagnetic. According to Fig. 6 (right inset), the MNPs were effectively attracted with an external magnet. These results show that the MNPs have excellent magnetic response, which prevents composite microspheres from aggregating and making them to redisperse rapidly in case of magnetic field removal.

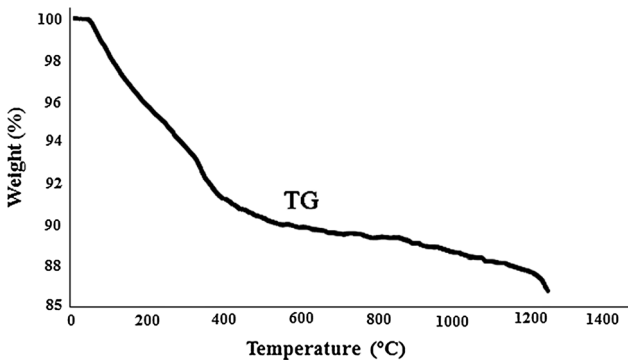


**Fig. 5** TG analysis spectra of the $Fe_3O_4$@$SiO_2$-$NH_2$/Cu(II)

## Catalytic synthesis of rhodanine and TZD derivatives

The catalytic properties of the $Fe_3O_4$@$SiO_2$-$NH_2$/Cu(II) catalyst were evaluated for the aldol condensation reaction between rhodanine or thiazolidine-2,4-dione and diverse aldehyde derivatives (Scheme 2).

In our initial experiments, a mixture of rhodanine or thiazolidine-2,4-dione (1 mmol), benzaldehyde (1 mmol), and catalyst (0.125 g) in ethanol under reflux conditions was stirred for a specified time, as required to complete the reaction (100 min). To optimize the conditions, the reaction was carried out in diverse solvents, using different temperatures. These experiments showed that ethanol is the most favorable solvent, due to its efficiency and environmental compatibility. Next, the quantity of catalyst was optimized (Table 1). In the absence of the catalyst, no product was detected and the starting materials were recovered. Optimal yields were obtained with 0.15 mg of the catalyst; higher amounts gave no further improvement. When aldehydes and rhodanine or thiazolidine-2,4-dione

**Scheme 2** Synthesis of rhodanine and TZD derivatives using $Fe_3O_4$@$SiO_2$-$NH_2$/Cu(II) Y = O, 2,4-thiazolidinedione; Y = S, rhodanine

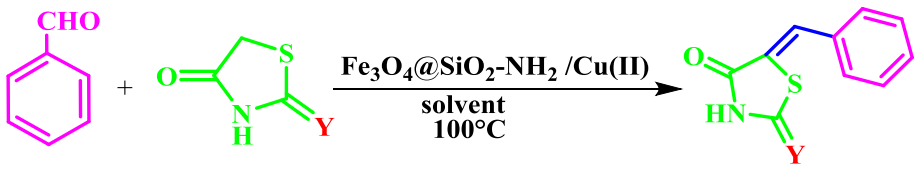


**Table 1** Aldol condensation of benzaldehyde (1 mmol), rhodanine and thiazolidine-2,4-dione (1 mmol) in the presence of $Fe_3O_4$@$SiO_2$-$NH_2$/Cu(II) under different condition

| Entry | Catalyst (g) | Y | Solvent | Temperature | Time (min) | Yield (%)[a] |
|---|---|---|---|---|---|---|
| 1 | – | O | – | Reflux | 300 | 0 |
| 2 | – | S | – | Reflux | 300 | 0 |
| 3 | 0.150 | O | EtOH | Reflux | 30 | 97 |
| 4 | 0.150 | S | EtOH | Reflux | 45 | 95 |
| 5 | 0.125 | O | EtOH | Reflux | 85 | 95 |
| 6 | 0.125 | S | EtOH | Reflux | 100 | 93 |
| 7 | 0.150 | O | $CH_3CN$ | Reflux | 160 | 79 |
| 8 | 0.150 | S | $CH_3CN$ | Reflux | 175 | 75 |
| 9 | 0.150 | O | methanol | Reflux | 150 | 78 |
| 10 | 0.150 | S | methanol | 100 °C | 170 | 76 |
| 11 | 0.125 | O | EtOH-$H_2O$ (1:1) | 100 °C | 250 | 25 |
| 12 | 0.125 | S | EtOH-$H_2O$ (1:1) | 100 °C | 250 | 20 |
| 13 | 0.150 | S | EtOH | Reflux | 30 | 85 |

[a] Isolated yields

were condensed under reflux in the presence of $Cu(OAc)_2$ as a homogeneous catalyst, the yield of product was 85% (Table 1, Entry 13).

Next, the effect of temperature was investigated, using 0.15 g of the catalyst (Table 1); reflux temperature was found to give the best results. Overall as shown in Table 1, the optimum yield was obtained using 0.15 g of catalyst, under reflux and in ethanol as solvent (entries 3 and 4; yield 97.0%)

With the optimized reaction conditions in hand, the reactions were explored with aromatic aldehydes containing both electron-withdrawing and releasing groups, heteroaromatic aldehydes, and aliphatic aldehydes (Table 2). All of these condensations gave very good yields, with reaction times ranging from 25 to 45 min.

A comparison of the results obtained in this study with some published procedures is given in Table 3. These results show that $Fe_3O_4$@$SiO_2$-$NH_2$/Cu(II) compares favorably, with high yields, short reaction times, and simple conditions.

The possible reaction pathway for the aldol condensation mediated by $Fe_3O_4$/$SiO_2$-NH-ligand-Cu(II) as a Lewis acid is outlined in Scheme 3. Electron deficient sites on the surface of the catalyst could coordinate with the O-donor sites of rhodanine or thiazolidine-2,4-dione and activate them for conversion to the enol form. Subsequent aldol type condensation leads to the corresponding product [7, 33].

**Table 2** Aldol condensation reaction catalyzed by $Fe_3O_4$@$SiO_2$-$NH_2$/Cu(II)

| Aldehyde | Y | Product | Yield (%) | M.p. reported |
|---|---|---|---|---|
| 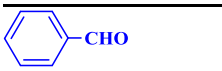 | O | 1a | 89 | 248–250 [26] |
| | S | 2a | 88 | 209–211 [26] |
| 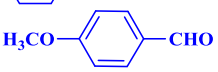 | O | 3b | 91 | 217–219 [26] |
| | S | 4b | 89 | 233–235 [26] |
| 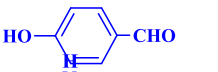 | O | 5c | 90 | >300 [26] |
| | S | 6c | 89 | 287–290 [26] |
| 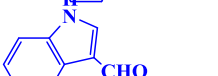 | O | 7d | 95 | 180–184 [27] |
| | S | 8d | 93 | 307–309 [27] |
| 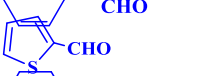 | O | 9e | 94 | 239 [27] |
| | S | 10e | 93 | 213–214 [27] |
| 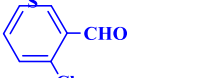 | O | 11f | 95 | 217–220 [26] |
| | S | 12f | 94 | 180–182 [26] |
| 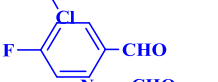 | O | 13g | 97 | 220–223 [26] |
| | S | 14g | 95 | 217–219 [26] |
| 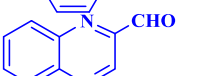 | O | 15h | 95 | Not reported |
| | S | 16 h | 94 | Not reported |
| 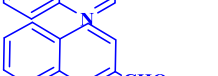 | 0 | 17i | 89 | 250–251 [28] |
| | S | 18i | 88 | 269–270 [28] |
| 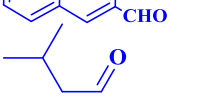 | O | 19j | 88 | Not reported |
| | S | 20j | 88 | 189 [29] |

**Table 3** Comparison of the catalytic activity of $Fe_3O_4$@$SiO_2$-$NH_2$/Cu(II) with other systems in the Knoevenagel condensation

| Entry | Catalyst/Conditions | Time (Min) | Yield (%) | Ref. |
|---|---|---|---|---|
| 1 | 2-HEAP[a]/solvent-free | 3–100 | 72–93 | [30] |
| 2 | Alum/microwave | 10–60 | 25–94 | [6] |
| 3 | Base/solvent | 360–780 | 50–90 | [9] |
| 4 | Toluene, Piperidine Reflux | 360 | 50–81 | [10] |
| 5 | [TMG][Lac][b]/80 °C | 20–120 | 85–94 | [7] |
| 6 | Pyridine/25–70 °C | 240–360 | 57–78 | [31] |
| 7 | $BiCl_3$/MW | 4–8 | 85–90 | [12] |
| 8 | Piperidine, HOAc/MW | 1.5 | 50–95 | [32] |
| 9 | $Fe_3O_4$@$SiO_2$-$NH_2$/Cu(II) | 20–60 | 88–97 | This work |

[a] 2-hydroxy ethylammonium propionate

[b] 1,1,3,3-tetramethylguanidine lactate

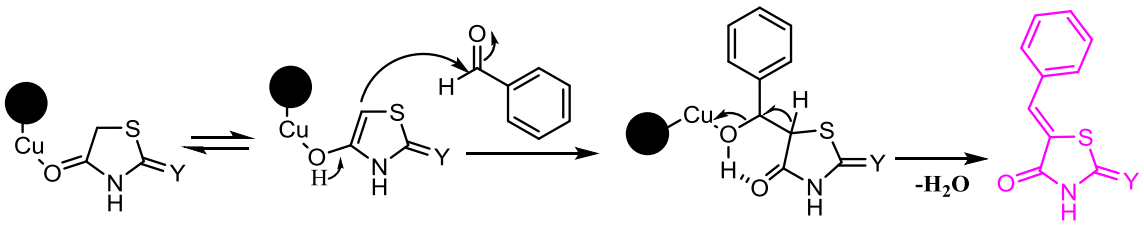


**Scheme 3** Plausible mechanism for aldol condensation in the presence $Cu^{2+}$ organocatalyst Y = O or S

**Table 4** Reusability of the $Fe_3O_4$@SiO2-NH2/Cu(II) MNPs for the synthesis of 5-arylidenthiazolidine-2,4-diones and 5-arylidene-2-thioxothiazolidin-4-one conclusion

| Cycle | 1st | 2nd | 3rd | 4th | 5th | 6th | 7th |
|---|---|---|---|---|---|---|---|
| Yield (%) | 98 | 98 | 96 | 94 | 93 | 92 | 90 |

We also evaluated the recoverability and reusability of this MNPs catalyst. After performance of the reaction, the catalyst was retrieved using an external magnet, washed twice with ethanol, and dried at 60 °C. The recovered catalyst was then reused in subsequent reactions. The catalyst could be retrieved up to seven times only a modest decrease in the yield of the reaction (Table 4); beyond this, the activity of the catalyst was reduced.

## Conclusion

We have described a rapid, green, and efficient method for the synthesis of rhodanine/thiazolidine-2,4-dione derivatives using a Cu(II) functionalized magnetic catalyst in ethanol under reflux conditions. The advantages of the present method are short reaction times, clean reaction profiles, reusability of the catalyst, mild reaction conditions, good yields, inexpensive and simple work-up of product, and green reaction conditions.

**Acknowledgements** The authors thankful the Mazandaran university of medical sciences for providing laboratory facilities to carry out this research.

## References

1. Jain AK, Vaidya A, Ravichandran V, Kashaw SK, Agrawal RK (2012) Bioorg Med Chem 20:3378–3395
2. Tomašić T, Peterlin Mašič L (2012) Expert Opin Drug Discov 7:549–560
3. Devinyak O, Zimenkovsky B, Lesyk R (2012) Curr Top Med Chem 12:2763–2784
4. Tomasic T, Masic LP (2009) Curr Med Chem 16:1596–1629
5. Johnson SL, Chen LH, Harbach R, Sabet M, Savinov A, Cotton NJ, Strongin A, Guiney D, Pellecchia M (2008) Chem Biol Drug Des 71:131–139
6. Shelke KF, Sapkal SB, Kakade GK, Sadaphal SA, Shingate BB, Shingare MS (2010) Green Chem Lett Rev 3:17–21
7. Sandhu JS (2013) Org Med Chem Lett 3:2
8. Metwally NH, Rateb NM, Zohdi HF (2011) Green Chem Lett Rev 4:225–228
9. Mahalle S, Ligampalle D, Mane R (2009) Heteroatom Chem 20:151–156
10. Bruno G, Costantino L, Curinga C, Maccari R, Monforte F, Nicolo F, Vigorita MG (2002) Bioorg Med Chem 10:1077–1084
11. Nitsche C, Klein CD (2012) Tetrahedron Lett 53:5197–5201
12. Shah S, Singh B (2012) Bioorg Med Chem Lett 22:5388–5391
13. Johnson JS, Evans DA (2000) Acc Chem Res 33:325–335

14. Jiang G, Gu X, Jiang G, Chen T, Zhan W, Tian S (2015) Sens Actuators 209:122–130
15. Corma A, Garcia H (2006) Adv Synth Catal 348:1391–1412
16. Gawande MB, Branco PS, Varma RS (2013) Chem Soc Rev 42:3371–3393
17. Narani A, Marella RK, Ramudu P, Rao KSR, Burri DR (2014) RSC Adv 4:3774–3781
18. Zhang F, Wu X, Liang C, Li X, Wang Z, Li H (2014) Green Chem 16:3768–3777
19. Balu AM, Baruwati B, Serrano E, Cot J, Garcia-Martinez J, Varma RS, Luque R (2011) Green Chem 13:2750–2758
20. Lu AH, Salabas EL, Schüth F (2007) Angew Chem Int Ed 46:1222–1244
21. Faraji M, Yamini Y, Rezaee M (2010) J Iran Chem Soc 7:1–37
22. Wagner AM, Knezevic CE, Wall JL, Sun VL, Buss JA, Allen LT, Wenzel AG (2012) Tetrahedron Lett 53:833–836
23. Wang H, Zhang W, Shentu B, Gu C, Weng Z (2012) J Appl Polym Sci 125:3730–3736
24. Shahbazi F, Amani K (2014) Catal Commun 55:57–64
25. Afradi M, Foroughifar N, Pasdar H, Moghanian H (2016) RSC Adv 64:59343–59351
26. Kumar B, Nanjan M, Suresh B, Karvekar M, Adhikary L (2006) J Heterocycl Chem 43:897–903
27. Riyaz S, Indrasena A, Naidu A, Dubey P (2014) Synth Commun 44:368–373
28. Russell AJ, Westwood IM, Crawford MH, Robinson J, Kawamura A, Redfield C, Laurieri N, Lowe ED, Davies SG, Sim E (2009) Bioorg Med Chem 17:905–918
29. Gränacher C, Gerö M, Ofner A, Klopfenstein A, Schlatter E (1923) Helv Chim Acta 6:458–467
30. Gong K, He Z-W, Xu Y, Fang D, Liu Z-L (2008) Monatsh Chem 139:913–915
31. Zvarec O, Polyak SW, Tieu W, Kuan K, Dai H, Pedersen DS, Morona R, Zhang L, Booker GW, Abell AD (2012) Bioorg Med Chem Lett 22:2720–2722
32. Drawanz BB, Ribeiro CS, Masteloto HG, Neuenfeldt PD, Pereira CM, Siqueira GM, Cunico W (2014) Ultrason Sonochem 21:1615–1617
33. Mobinikhaledi A, Foroughifar N, Khajeh-Amiri A (2016) React Kinet Mech Cat 117:59–75